IEEE Photonics Journal
An IEEE Photonics Society Publication

Open Access

A High-Speed and High-Sensitivity Photon-Counting Communication System Based on Multichannel SPAD Detection

Volume 13, Number 2, April 2021

Guanhua Wen
Jun Huang
Liang Zhang
Changkun Li
Tiancheng Wen
Jianyu Wang

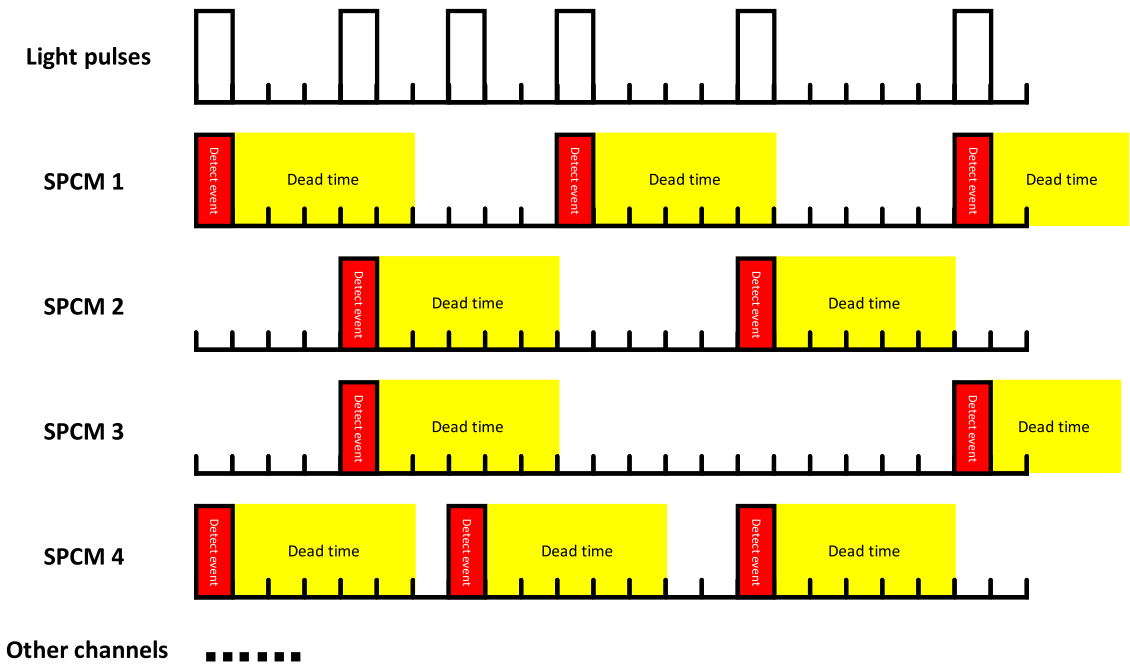

DOI: 10.1109/JPHOT.2021.3058002

A High-Speed and High-Sensitivity Photon-Counting Communication System Based on Multichannel SPAD Detection

Guanhua Wen,[1,2] Jun Huang,[1,2,3] Liang Zhang,[1,2] Changkun Li,[1] Tiancheng Wen,[1,2] and Jianyu Wang[1,4]

[1]Key Laboratory of Space Active Opto-Electronics Technology, Shanghai Institute of Technical Physics, Chinese Academy of Sciences, Shanghai 200083, China
[2]University of Chinese Academy of Sciences, Beijing 100049, China
[3]School of Information Science and Technology, ShanghaiTech University, Shanghai 201210, China
[4]Shanghai Quantum Science Research Center, Shanghai 201315, China

DOI:10.1109/JPHOT.2021.3058002

Manuscript received January 19, 2021; revised February 1, 2021; accepted February 4, 2021. Date of publication February 9, 2021; date of current version March 12, 2021. This work was supported by in part by the National Natural Science Foundation of China under Grant U1738204, in part by the Strategic Priority Research Program of the Chinese Academy of Sciences under Grant XDA22000000, in part by the Youth Innovation Promotion Association of Chinese Academy of Sciences, in part by the Shanghai Rising-Star Program under Grant 19QA1410400, and in part by the Shanghai Science and Technology Major Project under Grant 2019SHZDZX01. Corresponding authors: Liang Zhang; Jianyu Wang (e-mail: zhliang@mail.sitp.ac.cn; jywang@mail.sitp.ac.cn).

Abstract: In order to achieve high-speed, high-sensitivity optical communication over long distances and high attenuation channels, we propose a photon-counting communication system based on the detection of multichannel single-photon avalanche diodes (SPADs). First, the ideal pulse position modulation (PPM) bit error rate (BER) expression for a multichannel detection system is derived, and then the effect of the detector's dead time is taken into account. The BER of the multichannel detection system was analyzed by means of a Monte Carlo simulation, after which we set up a four-channel receiving experimental verification system with a 1×4 fiber splitter and four single-photon counting modules (SPCMs). The simulation and experimental results demonstrated that the BER of the multichannel detection system could be greatly reduced and the communication speed substantially improved. Finally, a reliable photon-counting communication system with a rate of 50 Mbps and sensitivity of 4 photons/bit was developed using serially-concatenated pulse position modulation (SCPPM) technology.

Index Terms: Photon-counting communication, single-photon counting module, multichannel detection, serially-concatenated pulse position modulation.

1. Introduction

In recent years, free space optical communication (FSO) has attracted much attention because of its unique features: large bandwidth, high data rate, less power, and low mass requirements. Many Gbps optical communication demonstration experiments have been carried out between earth orbiting satellites and ground stations [1]. However, with humans' ongoing exploration of outer space, such as the moon and Mars exploration missions, the communication distances are also increasing, and the optical signal intensity at the receiving end is also very weak, traditional

photodetectors can no longer meet the requirements of long distances and high attenuation links. A photon-counting communication system based on a single-photon detector has attracted significant attention in this field due to its higher detection sensitivity. In 2013, NASA conducted the Lunar Laser Communication Demonstration (LLCD) [2], by which high-speed laser communication between the moon and Earth was achieved. Moreover, further optical communication demonstrations are also planned, such as The Laser Communication Relay Demonstration (LCRD) [3], the Deep Space Optical Communication (DSOC) project [4], and the European Deep-Space Optical Communication System (DOCS) [5]; these missions are all intended to conduct optical communication experiments over very long distances. In LLCD, given the advantages of superconducting nanowire single-photon detectors (SNSPDs) [6], high quantum efficiency, short dead times, high-speed optical communication is easy to achieve; however, SNSPDs also have some disadvantages, such as high costs, large volume, and extremely low temperature conditions. Therefore, SNSPDs are not widely used at present, only used in some ground stations. For the deep space terminals and deep space relay satellites, single-photon avalanche diodes (SPADs) are a better choice.

The avalanche diode, when operated in Geiger mode, is also highly sensitive and can detect single photons, and is widely used in optical and quantum communication [7] due to its small size and simplicity of operation. Recently, there have been various studies on SPAD-based optical communication systems. Several studies in the literature [8]–[10] introduced underwater wireless optical communication systems based on SPADs. In [11], [12], a SPAD-based visible light communication system was introduced and a fast blind union detection algorithm was proposed. However, the bit widths of the above studies are relatively long (about 1 μs) and the number of pluses in the bit widths is used to distinguish bits "1" and "0," and therefore the transmission speed is not especially high. In our previous study [13], we investigated the photon-counting communication system with a short bit width, but the bit error rate (BER) was relatively high and the guard time was used to reduce the impacts of dead time, which also affects the communication speed.

In this study, we improved the detection method, and a multichannel detection scheme with a fiber splitter was used to reduce the BER and improve the communication rate. First, we theoretically deduced the ideal BER expression of the pulse position modulation (PPM) scheme based on multichannel detection. Then, considering the effect of dead time, the BER performance of the multichannel detection system was studied by means of a Monte Carlo simulation. Next, a four-channel experimental system was set up and a slot synchronization method was proposed. Finally, we investigated the coding gain of the serially-concatenated pulse position modulation (SCPPM). The results confirm that reliable communication is achievable with the SCPPM scheme.

2. Theoretical Analysis and Simulation

In this study, we adopt the PPM scheme. The M-order PPM divides a symbol into M slots, with only one slot possessing an optical pulse signal. This modulation scheme has a very high photon utilization efficiency and is highly suitable for power-restricted channels, such as deep space and deep-sea links.

2.1 Ideal Bit Error Rate Model

The ideal condition means that the detector only performs one detection at each slot, and the detection event of the current slot will not affect that of the other slots. Moreover, the detector we use is the commercial SPCM, which cannot distinguish the number of photons in one detection event.

Under the conditions of extremely weak light, the photons in the slot can be modeled as a Poisson process [14], and the probability of having k photons in the slot can be expressed as

$$P(k) = \frac{\lambda^k \cdot e^{-\lambda}}{k!} \tag{1}$$

where λ is the average number of photons in the slot. As the SPCM cannot distinguish the number of photons, the SPCM only has two outputs: "0" and "1." Thus, Eq.(1) can be converted into:

$$p(0) = e^{-\lambda}$$
$$p(1) = 1 - e^{-\lambda} \tag{2}$$

Let *ns* denote the signal photons in slot "1" and *nb* denote the noise photons. From this we derive the following equations:

$$p0(0|1) = e^{-(ns+nb)}$$
$$p0(1|1) = 1 - e^{-(ns+nb)}$$
$$p0(0|0) = e^{-nb}$$
$$p0(1|0) = 1 - e^{-nb} \tag{3}$$

where $p0(a|b)$ denotes the probability of outputting "a" in slot "b". If we have m receiving channels, the sum of m channel outputs can be expressed as

$$p(n|1) = C_m^n p0^n(1|1) p0^{m-n}(0|1) n = 0, 1, 2 \ldots m$$
$$p(n|0) = C_m^n p0^n(1|0) p0^{m-n}(0|0) n = 0, 1, 2 \ldots m \tag{4}$$

where $C_m^n = \frac{m!}{n!(m-n)!}$, $p(n|1)$ is the probability that n detectors detected photons in slot "1" and $p(n|0)$ is the probability that n detectors detected photons in slot "0." Then, we can obtain the cumulative distribution function in slots "1" and "0":

$$F0(n|1) = \sum_{x=0}^{n} p(x|1) = \sum_{x=0}^{n} C_m^x p0^x(1|1) p0^{m-x}(0|1) n = 0, 1, 2 \ldots m$$
$$F0(n|0) = \sum_{x=0}^{n} p(x|0) = \sum_{x=0}^{n} C_m^x p0^x(1|0) p0^{m-x}(0|0) n = 0, 1, 2 \ldots m \tag{5}$$

For an M-PPM symbol, there are M slots, only one of which is "1," and the others are "0." There are m detection channels, if n ($0 \le n \le m$) channels detect photons in slot "1," and there are also n ($0 \le n \le m$) channels detecting photons in l ($0 \le l \le M-1$) "0" slots, and in the other $M-1-l$ "0" slots, the number of channels that detected photons is less than n. The probability of this condition is as follows:

$$p_c = C_{M-1}^{l} p(n|1) p^l(n|0) F0^{M-1-l}(n-1|0) \tag{6}$$

The probability of the correct demodulation in this condition is $\frac{1}{l+1}$, and so the probability of correct demodulation of the PPM symbol can be obtained by summing all of the cases of n ($0 \le n \le m$) and l ($0 \le l \le M-1$):

$$ps_r = \sum_{l=0}^{M-1} \sum_{n=0}^{m} \frac{1}{l+1} p_c = \sum_{l=0}^{M-1} \frac{1}{l+1} C_{M-1}^{l} \sum_{n=0}^{m} p(n|1) p^l(n|0) F0^{M-1-l}(n-1|0) \tag{7}$$

(7) can be simplified as

$$ps_r = \frac{1}{M} \sum_{n=0}^{m} L(n) \left(F0^M(n|0) - F0^M(n-1|0) \right) \tag{8}$$

where $L(n) = \frac{p(n|1)}{p(n|0)}$, and therefore the probability of the symbol demodulation error is

$$ps_e = 1 - ps_r = 1 - \frac{1}{M} \sum_{n=0}^{m} L(n) \left(F0^M(n|0) - F0^M(n-1|0) \right) \tag{9}$$

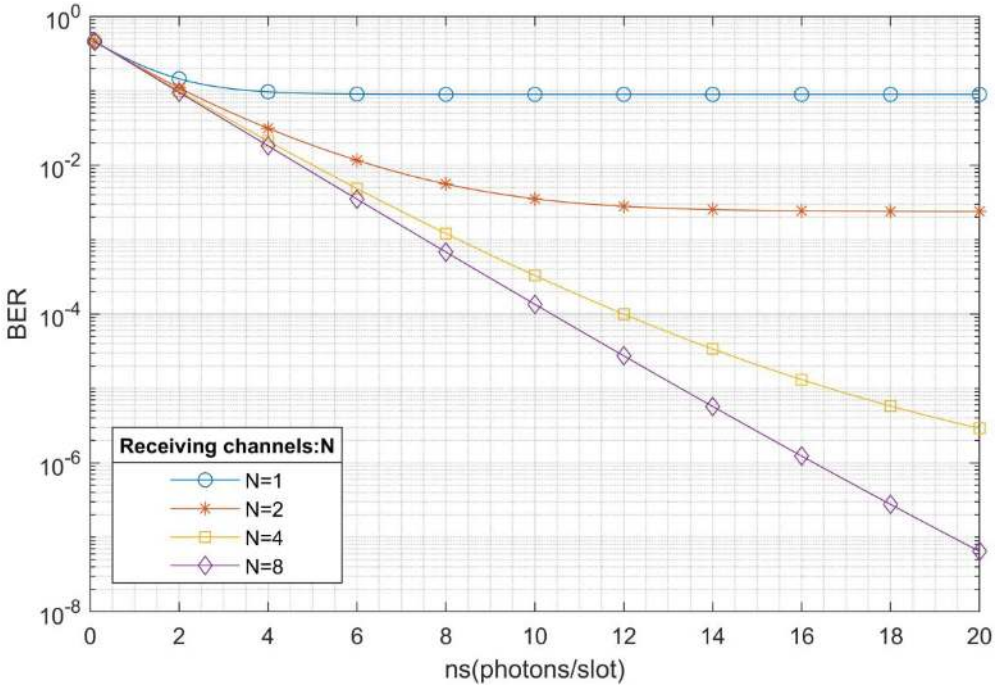

Fig. 1. Ideal BER performance with different receiving channels.

On average, a symbol error leads to $\frac{M \cdot \log_2 M}{2(M-1)}$ bit errors [15], and so the bit error probability of PPM demodulation can be expressed as follows:

$$pb_e = \frac{M}{2(M-1)} ps_e \tag{10}$$

In accordance with Eqs. (9) and (10), we can plot an ideal BER curve for a PPM optical communication system based on multichannel detection. Fig. 1 shows the 4 PPM BER performance under different receiving channels when the noise intensity is 0.1 photons/slot. As can be seen from the Fig. 1, the BER is lower with a multichannel system. As the signal intensity increases, the BER of four and eight channels can be reduced to a very low level. However, for the one-channel system, the BER has a lower bound [13], and will not decrease when it reaches this point.

2.2 Bit Error Rate Simulation Considering the Effect of Dead Time

In the above derivation, the dead time of the detector only influences the current slots, but has no effect on the other slots. In the actual detection, however, if the slot is very short or the dead time is long, other slots can also be influenced. The situation of multichannel detection, taking the influence of dead time into account, is shown in Fig. 2. After detecting a photon, the detector is unable to detect photons in the next slots in dead time; the multichannel detection method can alleviate this problem, when some detectors are in dead time, other detectors that are not in dead time can still work normally.

When considering the effect of dead time, the detection for each slot must take into consideration the detection situations of previous slots, and it is difficult to derive the expression of theoretical BER. In [16], the count rate of the SPAD under the influence of dead time was investigated, but this study mainly focused on how the count rate was affected by dead time and the slot widths in therein was 1 μs. In our study, however, the slot width is very short, totaling only 5 ns or even shorter, and the maximum count is one count at each slot. In this paper, therefore, the influence of dead time

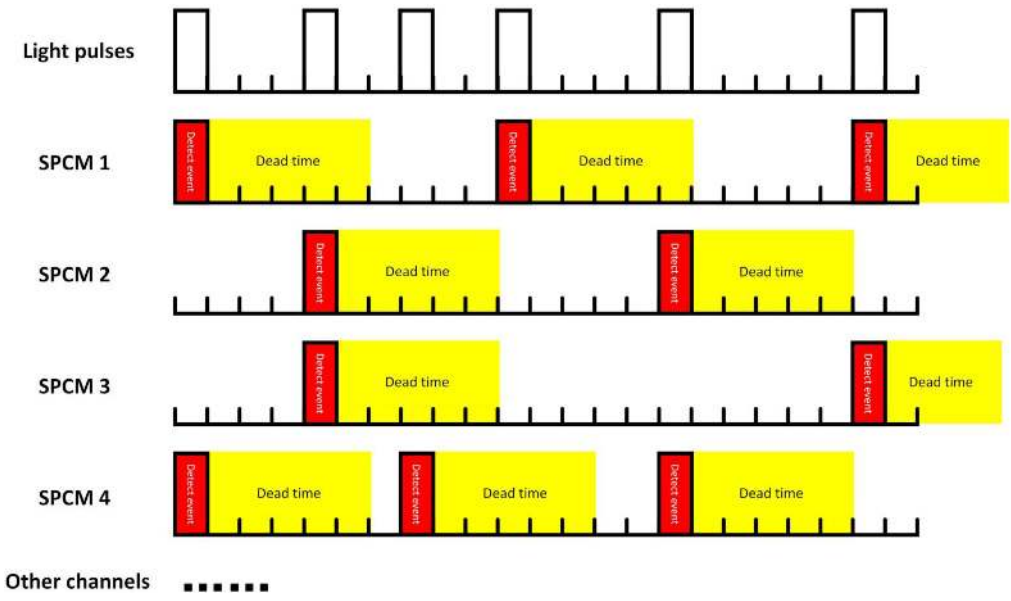

Fig. 2. Schematic diagram of multichannel detection.

was analyzed by means of a Monte Carlo simulation. We assume that the signal intensities in the different channels were equal. In order to simulate the effects of dead time, following a photon detection event, the detectors could not respond to photons in the subsequent slots which are in dead time, and, if the current slot is not in dead time, the outputs of the detectors obey the probability distribution in (3). The simulation results are shown in Fig. 3.

Fig. 3 shows the simulated BER with different receiving channels and dead time widths when the noise intensity was 0.1 photons/slot. As can be seen from the Fig. 3, the BER can be significantly reduced by utilizing the multichannel detection scheme. Meanwhile, by comparing the above four figures, it can also be noted that, as the slots become shorter, the impact of the dead time becomes greater and the BER increases accordingly. Another interesting finding was that, with the increase in the signal intensity, the BER decreased at first; as the signal intensity further increased, the BER also began to increase. This phenomenon would be more obvious if there were more receiving channels. The cause of this effect was that when the signal intensity becomes too high, all detectors detect photons, and so there are no longer detectors that can operate in the subsequent slots, because all the detectors are in dead time. Therefore, when using a multichannel detection scheme for optical communication, the signal intensity should be moderate, as too high or too low signal intensities will lead to an increase in the BER.

3. Experimental Setup

In order to verify the simulation results and prove the feasibility of the multichannel detection system, we built a four-channel photon-counting communication system using a 1×4 fiber splitter. The experimental system is shown in Fig. 4. First, a random sequence was generated and modulated on a PC, and then the modulated information was loaded into the arbitrary wave generator (Keysight, 81160a) by the Command Expert to drive a 780 nm laser (Fiblaser, FCM780S0LMP0) to generate the corresponding optical signal. Then, the optical signal was sent out via a collimating lens. After passing through some attenuation pieces, the optical signal was coupled to the fiber through a coupler. The power of the optical signal's intensity could be changed by an adjustable attenuator, whereas the noise intensity could be changed by changing the ambient light intensity. The optical signal was then divided into four channels by a 1×4 fiber splitter. Next, the four channels' optical

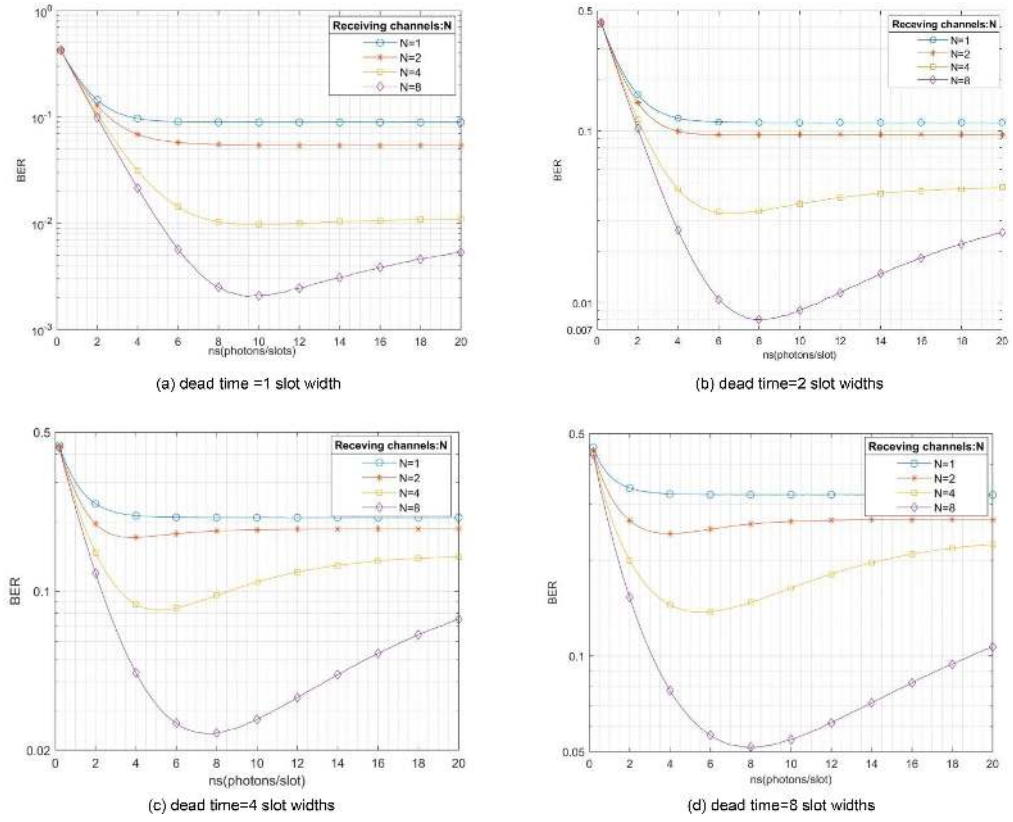

Fig. 3. Simulation results of the BER considering the effects of dead time.

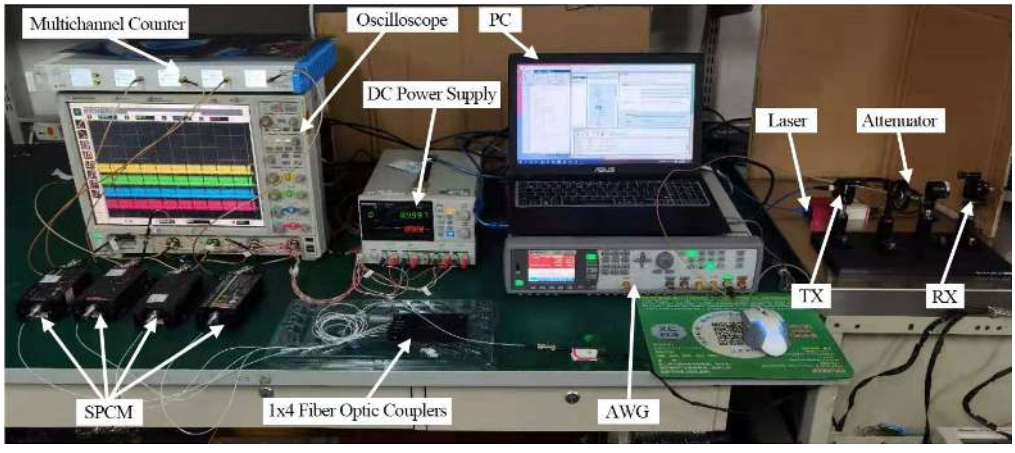

Fig. 4. Experimental system setup.

signals were detected by four SPCMs (Excelitas, SPCM-AQRH-13-FC). The outputs of the four detectors were connected to an oscilloscope (Agilent DSO9104A) and a multichannel counter (QuTAG), which were used for signal acquisition and light intensity estimation, respectively. The signals acquired by the oscilloscope were then transmitted to the PC. After the demodulation, we can obtain the BER by comparing the receiving sequence to the sending sequence. The specific parameters of the experiment are shown in Table 1.

TABLE 1
Experimental Parameters

Experimental parameters	
Laser wavelength	780nm
Slot width	5ns
Oscilloscope sampling rate	2GSa/s
Modulation mode	4PPM
SPCM parameters	
Dark count	170Hz
Dead time	28ns
Output pulse width	17.3ns
Detection efficiency	65%@780nm
After-pulse probability	0.2%

(a) (b)

Fig. 5. Received waveforms.

Because the light pulse width was 5 ns, four detectors may not detect photons simultaneously within a signal slot; one may detect them in the front of the pulse, and others may detect them at the end of the pulse. As is shown in Fig. 5(a), the rising edges of the four channels' pulses are not simultaneously generated. Therefore, an accurate slot synchronization method is necessary to determine which pulses belong to each slot. The slot synchronization method we employed here is similar to that cited in a previous study [10], in [10], a series of gated signals which had the same cycle but different offsets were used, and slot synchronization could be achieved by calculating the slot's maximum count value. In this study, the slots were very short and the output pulse width of detector was longer than the slot width, and so we needed to calculate the maximum sum of the four channels' pulse-increasing edges. The specific slot synchronization principle is shown in Fig. 6. We also added a synchronization sequence [17] prior to the signal sequence for frame synchronization, and utilized the frame synchronization state machine noted in the literature [18] to increase the reliability of the synchronization. After the synchronization had been completed, the maximum likelihood demodulation method was used. The BER can be obtained by comparing the receiving sequences with the sending ones.

The experimental results are shown in Fig. 7; in our experiments, the dead time of the SPCM was about 28 ns, the slot width was 5 ns, therefore the dead time was about six times slot widths. The simulation results are also plotted in Fig. 7, where the dead time was six slot widths. As can be seen in the Fig. 7, the four-channel system's experimental results were better than those

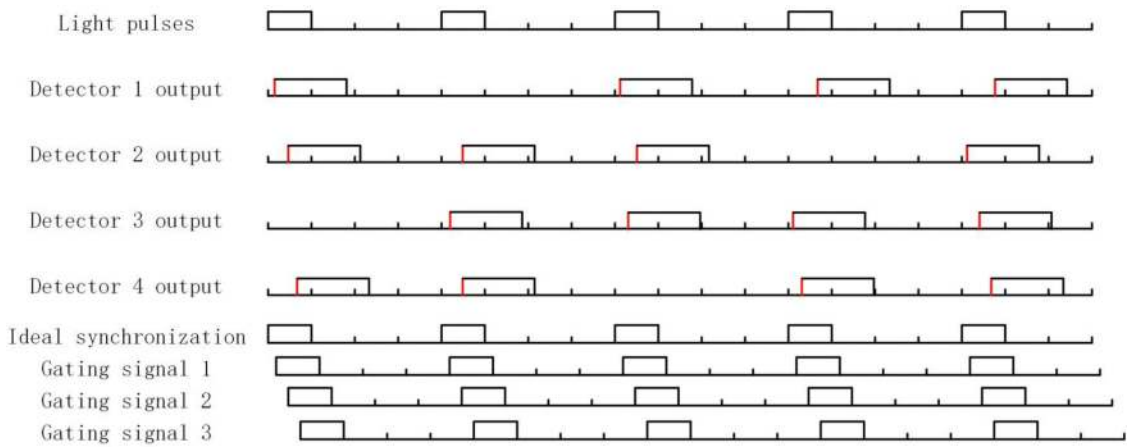

Fig. 6. Slot synchronization principle.

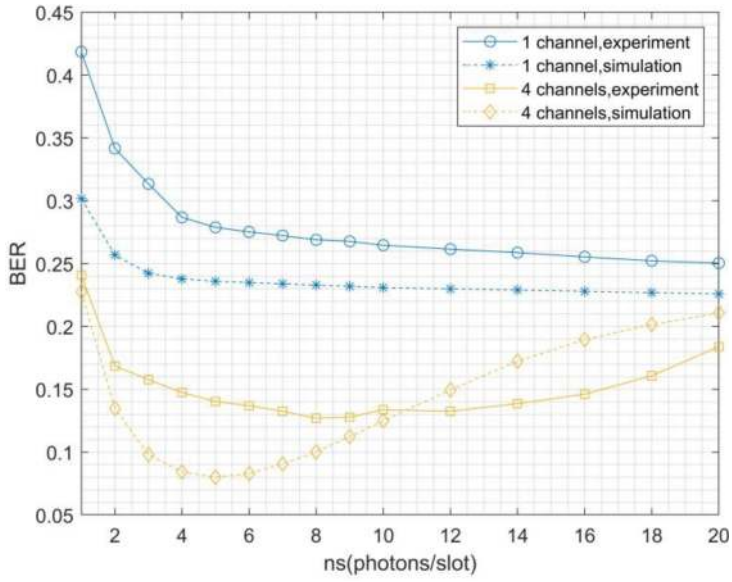

Fig. 7. Comparison of the experimental and simulation results.

from the one-channel configuration, and, with the increase in the signal intensity, the BER also initially decreased and increased when the signal intensity became too high. However, there are some differences between the experimental results and those of the simulation, with the best BER of the simulation results was about 8%, whereas the best BER of the experimental results was approximately 13%. This may be due to the following factors: 1) The conditions of the simulation were ideal detection conditions, as shown in Fig. 2, whereas those of the experiment were non-ideal, and which are shown in Fig. 5(a); 2) estimation of the signal intensity may not be accurate. Due to the influence of factors such as the after pulse and dark count, the observed counts may be larger than the actual ones, and it may be inaccurate to estimate the signal intensity by means of the pulse count rate and Poisson probability distribution. 3) Four channels' signal intensities were not exactly equal, and could also have led to differences between the experimental and simulation results.

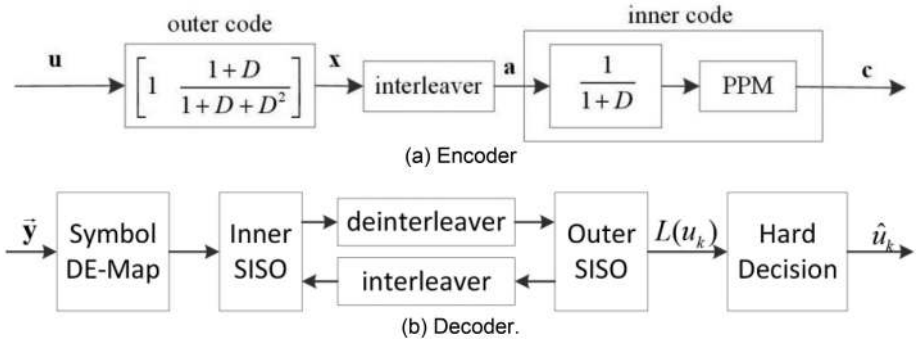

Fig. 8. Codec schematic diagram.

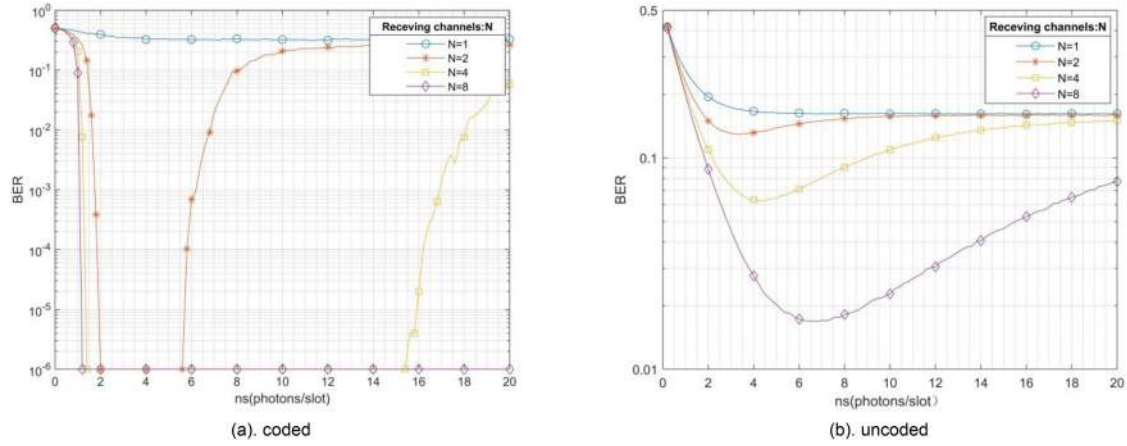

Fig. 9. BER comparison between coded and uncoded versions.

4. Serially-Concatenated Pulse Position Modulation

Although the BER could be reduced via the multichannel detection scheme, it was still too high to facilitate reliable communication. In order to further reduce it and achieve reliable communication, we employed error control coding technology. In this study, the SCPPM with a 1/2 code rate was adopted. This is an error-correcting coding scheme first proposed by NASA to support the Mars Laser Communications Demonstration project, which is able to maintain good error-correction performance under very low signal-to-noise ratio conditions. The schematic of the encoder is shown in Fig. 8(a), the decoder's schematic is shown in Fig. 8(b). The internal code decoding utilized the combined demodulation and decoding method noted in the literature [19], the outer code decoding method adopted the standard BCJR algorithm of the convolution code, and the internal and outer codes exchanged external information via the conventional turbo iteration.

We simulated the BER of the SCPPM under different receiving channels when the noise intensity was 0.01 photons/slot and the deadtime was four times slot widths. The coded simulation results are shown in Fig. 9(a), and the uncoded simulated results are shown in Fig. 9(b). By utilizing error control coding, the BER could be reduced to very low levels. Comparing Fig. 9(a) and (b), it can be seen that if the uncoded BER is below 15%, the BER can be reduced to 10^{-6} by means of encoding. The coded BER of the one-channel receiving system cannot be decreased because of a high uncoded BER, the coded BER of the four-channel receiving system can decrease to 10^{-6} when the signal intensity is moderate; however, when the signal intensity is too high, the increase in the uncoded BER will also result in an increase in the coded BER. In our experiment, when the

slot width is 5 ns, the best uncoded BER was about 13%, and therefore we can achieve reliable communication by utilizing SCPPM technology.

5. Conclusion

This study proposes a multichannel detection photon-counting system based on a fiber splitter. Through a theoretical analysis, simulation, and experimental verification, the multichannel detection system could significantly reduce the communication system's BER. Meanwhile, the effects of dead time can be mitigated by means of the multichannel receiving method, therefore the slots could be shorter and the communication speed could be higher. We also propose a synchronization technology that is suitable for multichannel detection systems. Finally, the SCPPM technology was adopted to achieve reliable communication. In our experiment, the slot width was 5 ns, each 4 PPM symbol could transmit 2 bits of information, and the code rate of the SCPPM was 1/2. Therefore, the final communication rate achieved was 50 Mbps. As can be seen in Fig. 7 and Fig. 9, when the signal intensity is 4 photons/slot, the BER of the experiment is below 15%, and the BER after coding can drop to below 10^{-6}. Therefore, the communication sensitivity was about 4 photons/bit. This paper provides a simple method for realizing a high-speed, high-sensitivity photon-counting communication system, which has important implications for optical communication technologies in outer space exploration.

References

[1] H. Kaushal and G. Kaddoum, "Optical communication in space: Challenges and mitigation techniques," *IEEE Commun. Surveys Tuts.,* vol. 19, no. 1, pp. 57–96, Jan. – Mar. 2016.

[2] D. M. Boroson *et al*., "Overview and results of the lunar laser communication demonstration," in *Free-Space Laser Communication Atmospheric Propagation XXVI*, vol. 8971, 2012.

[3] B. Edwards, D. Israel, and S. Vithlani, "Latest changes to NASA's laser communications relay demonstration project," in *Free-Space Laser Communicattion Atmospheric Propagation XXX*, vol. 10524, 2018.

[4] A. Biswas, M. Srinivasan, S. Piazzolla, and D. Hoppe, "Deep space optical communications," in *Free-Space Laser Communication Atmospheric Propagation XXX*, vol. 10524, 2018.

[5] Z. Sodnik, C. Heese, P. D. Arapoglou, K.-J. Schulz, I. Zayer, and R. J. Daddato, "European deep-space optical communication program," in *Free-Space Laser Communication and Atmospheric Propagation XXX*, vol. 10524, 2018.

[6] M. Grein *et al*., *A Superconducting Photon-Counting Receiver forOpt. Communication From Moon*. Bellingham, WA, USA: SPIE, 2015.

[7] S.-K. Liao *et al*., "Satellite-to-ground quantum key distribution," *Nature,* vol. 549, no. 7670, pp. 43–47, 2017.

[8] H. L. Chen *et al*., "Toward long-distance underwater wireless optical communication based on a high-sensitivity single photon avalanche diode," *IEEE Photon. J.,* vol. 12, no. 3, Jun. 2020, Art. no. 7902510.

[9] C. Wang, H.-Y. Yu, and Y.-J. Zhu, "A long distance underwater visible light communication system with single photon avalanche diode," *IEEE Photon. J.,* vol. 8, no. 5, Oct. 2016, Art. no. 7906311.

[10] Q. Yan, Z. Li, Z. Hong, T. Zhan, and Y. Wang, "Photon-counting underwater wireless optical communication by recovering clock and data from discrete single photon pulses," *IEEE Photon. J.,* vol. 11, no. 5, Oct. 2019, Art. no. 7905815.

[11] C. Wang, H.-Y. Yu, Y.-J. Zhu, T. Wang, and Y.-W. Ji, "Experimental study on SPAD-based VLC systems with an LED status indicator," *Opt. Exp.,* vol. 25, no. 23, pp. 28783–28793, 2017.

[12] Z. Tian, T. Wang, C. Wang, and Y. Zhu, "Experimental study on SPAD-based VLC systems after low-pass filtering," *Opt. Commun.,* vol. 434, pp. 253–256, 2019.

[13] G. H. Wen, J. Huang, J. S. Dai, L. Zhang, and J. Y. Wang, "Performance analysis optimization and experimental verification of a photon-counting communication system based on non-photon-number-resolution detectors," *Opt. Commun.,* vol. 468, pp. 125771–125778, 2020.

[14] S. O. Min, J. K. Hong, and T. H. Kim, "Systematic experiments for proof of poisson statistics on direct-detection laser radar using geiger mode avalanche photodiode," *Curr. Appl. Phys.,* vol. 10, no. 4, pp. 1041–1045, 2010.

[15] J. Abshire, "Performance of OOK and low-order PPM modulations in optical communications when using APD-Based receivers," *IEEE Trans. Commun.,* vol. 32, no. 10, pp. 1140–1143, Oct. 2003.

[16] E. Sarbazi, M. Safari, and H. Haas, "Photon detection characteristics and error performance of SPAD array optical receivers," in *Proc. 4th Int. Workshop Opt. Wireless Commun*., 2015, pp. 132–136.

[17] R. Gagliardi, J. Robbins, and H. Taylor, "Acquisition sequences in PPM communications (Corresp.)," *IEEE Trans. Inf. Theory,* vol. IT-33, no. 5, pp. 738–744, Sep. 1987.

[18] Y. Tu *et al*., "Frame synchronization of pulse position modulation in high-speed optical communication with variable threshold," *Chin. J. Lasers,* vol. 44, no. 11, pp. 1106008–1–1106008–8, 2017, Art. no. 0258-7025 (2017).

[19] B. Moision and J. Hamkins, "Coded modulation for the deep-space optical channel: Serially concatenated pulse-position modulation," *Devlop. Biol.,* vol. 283, no. 1, pp. 113–127, 2005.